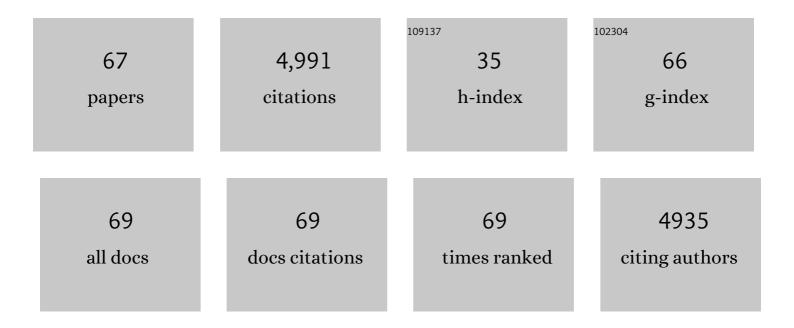
Matthew Ginder-Vogel

List of Publications by Year in descending order

Source: https://exaly.com/author-pdf/2004151/publications.pdf Version: 2024-02-01



#	Article	IF	CITATIONS
1	Isotopic analysis of radium geochemistry at discrete intervals in the Midwestern Cambrian-Ordovician aquifer system. Applied Geochemistry, 2022, 142, 105300.	1.4	3
2	Strontium and radium occurrence at the boundary of a confined aquifer system. Applied Geochemistry, 2022, 142, 105332.	1.4	5
3	Association of Radionuclide Isotopes with Aquifer Solids in the Midwestern Cambrian–Ordovician Aquifer System. ACS Earth and Space Chemistry, 2021, 5, 268-278.	1.2	3
4	Simultaneous Kinetics of Selenite Oxidation and Sorption on δ-MnO2 in Stirred-Flow Reactors. International Journal of Environmental Research and Public Health, 2021, 18, 2902.	1.2	3
5	Selective Reactivity and Oxidation of Dissolved Organic Matter by Manganese Oxides. Environmental Science & Technology, 2021, 55, 12084-12094.	4.6	36
6	Investigation of ICPâ€MS/MS for total sulfur quantification in freshwater dissolved organic matter. Journal of Environmental Quality, 2021, 50, 1476-1485.	1.0	5
7	Recycled concrete aggregate in base course applications: Review of field and laboratory investigations of leachate pH. Journal of Hazardous Materials, 2020, 385, 121562.	6.5	28
8	Effects of Co(II) ion exchange, Ni(II)- and V(V)-doping on the transformation behaviors of Cr(III) on hexagonal turbostratic birnessite-water interfaces. Environmental Pollution, 2020, 256, 113462.	3.7	17
9	Organic structure and solid characteristics determine reactivity of phenolic compounds with synthetic and reclaimed manganese oxides. Environmental Science: Water Research and Technology, 2020, 6, 540-553.	1.2	14
10	Identifying the mechanisms of cation inhibition of phenol oxidation by acid birnessite. Journal of Environmental Quality, 2020, 49, 1644-1654.	1.0	5
11	Impact of Dissolved Organic Matter on Porewater Hg and MeHg Concentrations in St. Louis River Estuary Sediments. ACS Earth and Space Chemistry, 2020, 4, 1386-1397.	1.2	6
12	Neutralization of high pH and alkalinity effluent from recycled concrete aggregate by common subgrade soil. Journal of Environmental Quality, 2020, 49, 172-183.	1.0	10
13	Spatial and temporal variability of radium in the Wisconsin Cambrian–Ordovician aquifer system. AWWA Water Science, 2020, 2, e1171.	1.0	7
14	Impact of bisphenol A influent concentration and reaction time on MnO ₂ transformation in a stirred flow reactor. Environmental Sciences: Processes and Impacts, 2019, 21, 19-27.	1.7	15
15	Characterization of Recycled Concrete Aggregate after Eight Years of Field Deployment. Journal of Materials in Civil Engineering, 2019, 31, .	1.3	9
16	Dual Role of Humic Substances As Electron Donor and Shuttle for Dissimilatory Iron Reduction. Environmental Science & Technology, 2018, 52, 5691-5699.	4.6	116
17	Coordination geometry of Zn2+ on hexagonal turbostratic birnessites with different Mn average oxidation states and its stability under acid dissolution. Journal of Environmental Sciences, 2018, 65, 282-292.	3.2	13
18	Changes in oxidative potential of soil and fly ash after reaction with gaseous nitric acid. Atmospheric Environment, 2018, 173, 306-315.	1.9	9

MATTHEW GINDER-VOGEL

#	Article	IF	CITATIONS
19	Stability of Ferrihydrite–Humic Acid Coprecipitates under Iron-Reducing Conditions. Environmental Science & Technology, 2018, 52, 13174-13183.	4.6	31
20	Use of Routine Soil Tests to Estimate Pb Bioaccessibility. Environmental Science & Technology, 2018, 52, 12556-12562.	4.6	7
21	Effect of geochemical conditions on radium mobility in discrete intervals within the Midwestern Cambrian-Ordovician aquifer system. Applied Geochemistry, 2018, 97, 238-246.	1.4	6
22	Decreased Electron Transfer between Cr(VI) and AH ₂ DS in the Presence of Goethite. Journal of Environmental Quality, 2018, 47, 139-146.	1.0	2
23	Arsenite Depletion by Manganese Oxides: A Case Study on the Limitations of Observed First Order Rate Constants. Soil Systems, 2018, 2, 39.	1.0	20
24	The reactivity of Fe(II) associated with goethite formed during short redox cycles toward Cr(VI) reduction under oxic conditions. Chemical Geology, 2017, 464, 101-109.	1.4	38
25	Structural Transformation of MnO ₂ during the Oxidation of Bisphenol A. Environmental Science & Technology, 2017, 51, 6053-6062.	4.6	86
26	Colonization Habitat Controls Biomass, Composition, and Metabolic Activity of Attached Microbial Communities in the Columbia River Hyporheic Corridor. Applied and Environmental Microbiology, 2017, 83, .	1.4	20
27	Local structure of Cu2+ in Cu-doped hexagonal turbostratic birnessite and Cu2+ stability under acid treatment. Chemical Geology, 2017, 466, 512-523.	1.4	31
28	The role of dissolved Fe(II) concentration in the mineralogical evolution of Fe (hydr)oxides during redox cycling. Chemical Geology, 2016, 438, 163-170.	1.4	41
29	Influence of Oxygen and Nitrate on Fe (Hydr)oxide Mineral Transformation and Soil Microbial Communities during Redox Cycling. Environmental Science & Technology, 2016, 50, 3580-3588.	4.6	101
30	The Presence of Ferrihydrite Promotes Abiotic Formation of Manganese (Oxyhydr)oxides. Soil Science Society of America Journal, 2015, 79, 1297-1305.	1.2	35
31	Formation and secondary mineralization of ferrihydrite in the presence of silicate and Mn(II). Chemical Geology, 2015, 415, 37-46.	1.4	52
32	A critical review of the reactivity of manganese oxides with organic contaminants. Environmental Sciences: Processes and Impacts, 2014, 16, 1247.	1.7	213
33	Effects of Co and Ni co-doping on the structure and reactivity of hexagonal birnessite. Chemical Geology, 2014, 381, 10-20.	1.4	66
34	Arsenite modifies structure of soil microbial communities and arsenite oxidization potential. FEMS Microbiology Ecology, 2013, 84, 270-279.	1.3	25
35	Chromium(III) Oxidation by Three Poorly-Crystalline Manganese(IV) Oxides. 1. Chromium(III)-Oxidizing Capacity. Environmental Science & Technology, 2012, 46, 11594-11600.	4.6	80
36	Chromium(III) Oxidation by Three Poorly Crystalline Manganese(IV) Oxides. 2. Solid Phase Analyses. Environmental Science & Technology, 2012, 46, 11601-11609.	4.6	43

#	Article	IF	CITATIONS
37	Structural study of biotic and abiotic poorly-crystalline manganese oxides using atomic pair distribution function analysis. Geochimica Et Cosmochimica Acta, 2012, 81, 39-55.	1.6	68
38	Synthesis and evaluation of substrate analogue inhibitors of trypanothione reductase. Journal of Enzyme Inhibition and Medicinal Chemistry, 2012, 27, 784-794.	2.5	10
39	Speciation and Release Kinetics of Cadmium in an Alkaline Paddy Soil under Various Flooding Periods and Draining Conditions. Environmental Science & amp; Technology, 2011, 45, 4249-4255.	4.6	191
40	Arsenite Oxidation by a Poorly-Crystalline Manganese Oxide. 3. Arsenic and Manganese Desorption. Environmental Science & Technology, 2011, 45, 9218-9223.	4.6	100
41	Responses of microbial community functional structures to pilot-scale uranium <i>in situ</i> bioremediation. ISME Journal, 2010, 4, 1060-1070.	4.4	98
42	Significant Association between Sulfate-Reducing Bacteria and Uranium-Reducing Microbial Communities as Revealed by a Combined Massively Parallel Sequencing-Indicator Species Approach. Applied and Environmental Microbiology, 2010, 76, 6778-6786.	1.4	102
43	Biogeochemical Redox Processes and their Impact on Contaminant Dynamics. Environmental Science & Technology, 2010, 44, 15-23.	4.6	1,037
44	Arsenite Oxidation by a Poorly Crystalline Manganese-Oxide. 2. Results from X-ray Absorption Spectroscopy and X-ray Diffraction. Environmental Science & Technology, 2010, 44, 8467-8472.	4.6	181
45	Ni(II) Sorption on Biogenic Mn-Oxides with Varying Mn Octahedral Layer Structure. Environmental Science & Technology, 2010, 44, 4472-4478.	4.6	79
46	Arsenite Oxidation by a Poorly Crystalline Manganese-Oxide 1. Stirred-Flow Experiments. Environmental Science & Technology, 2010, 44, 8460-8466.	4.6	179
47	Molecular Scale Assessment of Methylarsenic Sorption on Aluminum Oxide. Environmental Science & Technology, 2010, 44, 612-617.	4.6	45
48	Kinetics of Chromium(III) Oxidation by Manganese(IV) Oxides Using Quick Scanning X-ray Absorption Fine Structure Spectroscopy (Q-XAFS). Environmental Science & Technology, 2010, 44, 143-149.	4.6	72
49	Formation of nano-crystalline todorokite from biogenic Mn oxides. Geochimica Et Cosmochimica Acta, 2010, 74, 3232-3245.	1.6	93
50	The Impacts of X-Ray Absorption Spectroscopy on Understanding Soil Processes and Reaction Mechanisms. Developments in Soil Science, 2010, 34, 1-26.	0.5	13
51	Kinetic and Mechanistic Constraints on the Oxidation of Biogenic Uraninite by Ferrihydrite. Environmental Science & Technology, 2010, 44, 163-169.	4.6	60
52	Cation Effects on the Layer Structure of Biogenic Mn-Oxides. Environmental Science & Technology, 2010, 44, 4465-4471.	4.6	126
53	Quantification of rapid environmental redox processes with quick-scanning x-ray absorption spectroscopy (Q-XAS). Proceedings of the National Academy of Sciences of the United States of America, 2009, 106, 16124-16128.	3.3	84
54	Effects of gamma-sterilization on the physico-chemical properties of natural sediments. Chemical Geology, 2008, 251, 1-7.	1.4	59

#	Article	IF	CITATIONS
55	Microbial Communities in Contaminated Sediments, Associated with Bioremediation of Uranium to Submicromolar Levels. Applied and Environmental Microbiology, 2008, 74, 3718-3729.	1.4	154
56	Decreasing Lead Bioaccessibility in Industrial and Firing Range Soils with Phosphateâ€Based Amendments. Journal of Environmental Quality, 2008, 37, 2116-2124.	1.0	24
57	XANES Spectroscopic Analysis of Phosphorus Speciation in Alumâ€Amended Poultry Litter. Journal of Environmental Quality, 2008, 37, 477-485.	1.0	47
58	Elucidating Biogeochemical Reduction of Chromate via Carbon Amendments and Soil Sterilization. Geomicrobiology Journal, 2007, 24, 125-132.	1.0	7
59	Chapter 11 Biogeochemical Uranium Redox Transformations: Potential Oxidants of Uraninite. Developments in Earth and Environmental Sciences, 2007, , 293-319.	0.1	8
60	In Situ Bioreduction of Uranium (VI) to Submicromolar Levels and Reoxidation by Dissolved Oxygen. Environmental Science & Technology, 2007, 41, 5716-5723.	4.6	182
61	Micro-Scale Heterogeneity in Biogeochemical Uranium Cycling. AIP Conference Proceedings, 2007, , .	0.3	0
62	Hyperaccumulator <i>Alyssum murale</i> relies on a different metal storage mechanism for cobalt than for nickel. New Phytologist, 2007, 175, 641-654.	3.5	171
63	Thermodynamic Constraints on the Oxidation of Biogenic UO2by Fe(III) (Hydr)oxides. Environmental Science & Technology, 2006, 40, 3544-3550.	4.6	129
64	Heterogeneous response to biostimulation for U(VI) reduction in replicated sediment microcosms. Biodegradation, 2006, 17, 303-316.	1.5	55
65	Pilot-Scale in Situ Bioremedation of Uranium in a Highly Contaminated Aquifer. 2. Reduction of U(VI) and Geochemical Control of U(VI) Bioavailability. Environmental Science & Technology, 2006, 40, 3986-3995.	4.6	242
66	Chromate Reduction and Retention Processes within Arid Subsurface Environments. Environmental Science & Technology, 2005, 39, 7833-7839.	4.6	41
67	Bioreduction of Uranium in a Contaminated Soil Column. Environmental Science & Technology, 2005, 39, 4841-4847.	4.6	133